



Preliminary Results of a RANS Simulation for a Floating Point Absorber Wave Energy System Under Extreme Wave Conditions

Y. Yu and Y. Li

*Presented at the 30th International Conference on Ocean, Offshore, and Arctic Engineering
Rotterdam, The Netherlands
June 19 – 24, 2011*

NREL is a national laboratory of the U.S. Department of Energy, Office of Energy Efficiency & Renewable Energy, operated by the Alliance for Sustainable Energy, LLC.

Conference Paper
NREL/CP-5000-50967
October 2011

Contract No. DE-AC36-08GO28308

NOTICE

The submitted manuscript has been offered by an employee of the Alliance for Sustainable Energy, LLC (Alliance), a contractor of the US Government under Contract No. DE-AC36-08GO28308. Accordingly, the US Government and Alliance retain a nonexclusive royalty-free license to publish or reproduce the published form of this contribution, or allow others to do so, for US Government purposes.

This report was prepared as an account of work sponsored by an agency of the United States government. Neither the United States government nor any agency thereof, nor any of their employees, makes any warranty, express or implied, or assumes any legal liability or responsibility for the accuracy, completeness, or usefulness of any information, apparatus, product, or process disclosed, or represents that its use would not infringe privately owned rights. Reference herein to any specific commercial product, process, or service by trade name, trademark, manufacturer, or otherwise does not necessarily constitute or imply its endorsement, recommendation, or favoring by the United States government or any agency thereof. The views and opinions of authors expressed herein do not necessarily state or reflect those of the United States government or any agency thereof.

Available electronically at <http://www.osti.gov/bridge>

Available for a processing fee to U.S. Department of Energy and its contractors, in paper, from:

U.S. Department of Energy
Office of Scientific and Technical Information

P.O. Box 62
Oak Ridge, TN 37831-0062
phone: 865.576.8401
fax: 865.576.5728
email: <mailto:reports@adonis.osti.gov>

Available for sale to the public, in paper, from:

U.S. Department of Commerce
National Technical Information Service
5285 Port Royal Road
Springfield, VA 22161
phone: 800.553.6847
fax: 703.605.6900
email: orders@ntis.fedworld.gov
online ordering: <http://www.ntis.gov/help/ordermethods.aspx>

Cover Photos: (left to right) PIX 16416, PIX 17423, PIX 16560, PIX 17613, PIX 17436, PIX 17721



Printed on paper containing at least 50% wastepaper, including 10% post consumer waste.

PRELIMINARY RESULTS OF A RANS SIMULATION FOR A FLOATING POINT ABSORBER WAVE ENERGY SYSTEM UNDER EXTREME WAVE CONDITIONS

Yi-Hsiang Yu

National Renewable Energy Laboratory (NREL)
National Wind Technology Center
Golden, CO 80041
Email: yi-hsiang.yu@nrel.gov

Ye Li

National Renewable Energy Laboratory (NREL)
National Wind Technology Center
Golden, CO 80041
Email: ye.li@nrel.gov

ABSTRACT

This paper presents the results of a preliminary study on the hydrodynamics of a moored floating-point absorber (FPA) wave energy system under extreme wave conditions. For this study, we assumed that the FPA is locked in harsh weather conditions, and the whole device moves as a single rigid body. The prediction of the hydrodynamic response of the system and the corresponding wave impact loads on the FPA are important to the structural design of the system and its survivability in extreme wave conditions.

After describing the working principle and the design specification of the floating-point absorber, we present the Reynolds-Averaged Navier-Stokes (RANS) method used in the study. We apply this method to analyze the hydrodynamic response of the FPA in regular as well as irregular waves. In addition, we evaluate the feasibility of using a Morison's Equation method for modeling the FPA system. Overall, the study shows that the nonlinear interaction between waves and the moored absorber has significant influences on the absorber response under extreme wave conditions.

KEYWORDS

Wave energy conversion (WEC); Reynolds-Averaged Navier-Stokes (RANS) equation; degree of freedom (DOF); volume of fluid (VOF); free surface; floating-point absorber (FPA)

INTRODUCTION

Ocean waves contain a significant amount of renewable energy [1]. A wide variety of wave energy conversion devices have been developed based on various technologies and theories to capture the energy. These devices include oscillating

water columns, overtopping devices, floating pitching devices, bottom-hinge devices, and FPAs. Comprehensive reviews on the fundamental designs and operating principles of wave energy systems can be found in [2,3]. The FPA is one of the simplest and one of the most promising WEC devices among numerous designs. This paper focuses on the study of a FPA system.

The FPA is typically a single buoy that either reacts against the seabed or a two-body system that generates energy from the relative motion between the two bodies. An example of the two-body FPA system is Ocean Power Technology's (OPT's) 40-kW utility-scale PowerBuoy. OPT deployed two of these systems, one in Santona Spain in 2008 and the other in Ohau Hawaii in 2009 (Fig. 1).



FIGURE 1. A PROTOTYPE OF OPT'S POWERBUOY WAVE ENERGY GENERATION SYSTEM (NREL PIX 17114)

In 1970s, FPA research focused on understanding the complex hydrodynamics of FPA devices and on the prediction of the maximum wave power absorption [4,5,6,7]. These theoretical studies were reviewed by Falnes in [8,9]. More recent studies have focused on improving wave extraction efficiency under various wave conditions, using hydraulic power take off (PTO) mechanisms and latching control [10]. The studies have also examined optimal control strategies for irregular sea waves [11] and the use of array systems [12,13].

Most of the numerical analyses on wave energy system efficiency were performed using frequency domain potential flow methods for calculating the hydrodynamic excitation forces (e.g. [11,13,14,15,16]). However, the non-linear interaction between waves and a WEC device was assumed to be small in those studies, thus the wave breaking and overtopping effects were not considered. A more comprehensive understanding of the FPA system may require the use of more advanced numerical methods such as the RANS method. An example of the RANS analysis is presented in [17], in which the hydrodynamics of cylinder type buoys and the power capture efficiency were analyzed. In our related work, we performed a series of analyses using the RANS method to understand a practical FPA system. We investigated the hydrodynamics of a two-body FPA system and its power absorption efficiency under given conditions [18].

The objective of this research is to analyze the hydrodynamics of a FPA wave energy system in extreme wave conditions. First we present the working principle and the design specification. We modeled the baseline mooring configuration and the hydrodynamic response of the FPA using a Morison's type method (OrcaFlex). We then investigated the flow field around the moored FPA and its hydrodynamic response in regular and irregular waves as well as the wave loads on the FPA body using the RANS method.

POINT WAVE ABSORBER MODEL

The point wave absorber model contains a float and a reaction part that includes a central column and a reaction plate. For extreme wave conditions, we assumed the absorber to be locked, and we performed the numerical study assuming all the parts are moving together as a single rigid body.

We first designed the model using SolidWork, and then further modified the geometry in the numerical modeling by keeping the center of buoyancy, B, as close as to the original SolidWork design. The model properties and the dimensions are shown in Tab. 1 and Fig. 2, respectively, where G is the center of gravity, and the metacentric M is calculated by following

$$\begin{aligned} BM &= I / \nabla, \\ GM &= OG - OB + BM, \end{aligned} \quad (1)$$

where O is located at the intersection of the mean free surface and the longitudinal axis of the FPA, I is the area of inertia, and ∇ is the displacement of the model.

TABLE 1. POINT WAVE ABSORBER MODEL PROPERTIES

Model properties	Values (unit)
Center of gravity G	22.4 (m) below the mean free surface
Center of Buoyancy B	1.17 (m) above G
Moment of inertia for pitch	69300 (kg m ²)
Metacentric M	4.12 (m) above G
Weight	250 (metric tons)

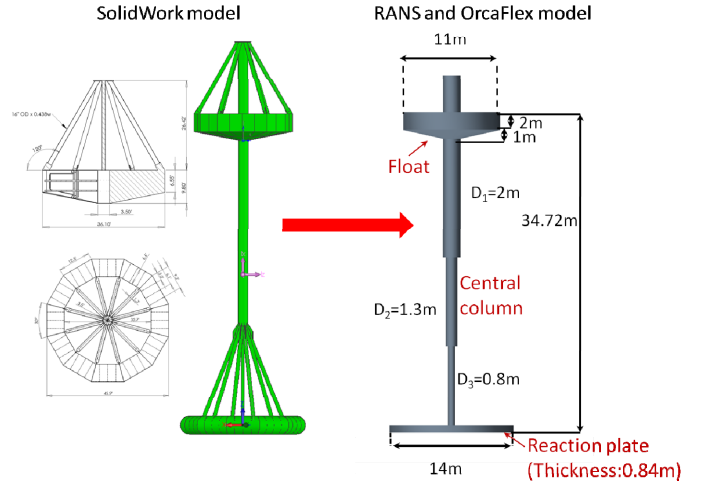


FIGURE 2. FPA GEOMETRY AND DIMENSIONS

MODELING

RANS method

We applied a finite volume method-based RANS model (StarCCM+) for solving the details of the unsteady incompressible flow field around the FPA. The continuity equation and the Navier-Stokes equations are given as

$$\begin{aligned} \nabla \cdot \mathbf{U} &= 0, \\ \rho(\mathbf{U}_t + \mathbf{U} \cdot \nabla \mathbf{U}) &= -\nabla p + \mathbf{F}_b + \nabla \cdot \mathbf{T} \end{aligned} \quad (2)$$

where ρ is the water density, \mathbf{U} is the flow velocity vector, and \mathbf{U}_t is its time derivative, \mathbf{F}_b is the body force vector (e.g., gravity), and \mathbf{T} is the stress tensor.

The governing equations are discretized over the computational domain and are solved using a transient SIMPLE for the pressure-velocity coupling. The set of linear equations is solved through the use of an algebraic multigrid method. A $k-\omega$ SST turbulence model is applied with a two-layer all y^+ wall treatment model, and the unsteady simulation is performed using a second order implicit scheme for time marching. The water free surface is captured using a volume of fluid (VOF) method, and a morphing model is adopted to move the mesh, where the cell movement and its deformation are taken into account in the momentum equation using an arbitrary Lagrangian-Eulerian method.

Absorber response calculation

The translation and rotation of the body of the body (Fig. 3) is calculated by solving the equation of motion after the excitation force is obtained, and the equation of motion calculation is coupled with the RANS simulation. The translation and the rotation of the body at the center of gravity are solved following

$$\begin{aligned} \mathbf{F} &= m_b \mathbf{a}_t, \\ \mathbf{M} &= \mathbf{I}_g \mathbf{a}_\Omega + \boldsymbol{\Omega} \times \mathbf{I}_g \boldsymbol{\Omega}, \end{aligned} \quad (3)$$

where m_b is the mass of the body, \mathbf{a}_t is the acceleration vector for the translation, $\boldsymbol{\Omega}$ and \mathbf{a}_Ω are the angular velocity and acceleration vectors, \mathbf{I}_g is the moment of inertia tensor at the center of gravity, \mathbf{F} and \mathbf{M} are the resulting force and moment acting on the body, including the buoyancy force, wave load and the weight of the body. The corresponding translational and rotational motions are calculated by integrating the accelerations over time, and the equation of motion is coupled with the RANS method through iterations.

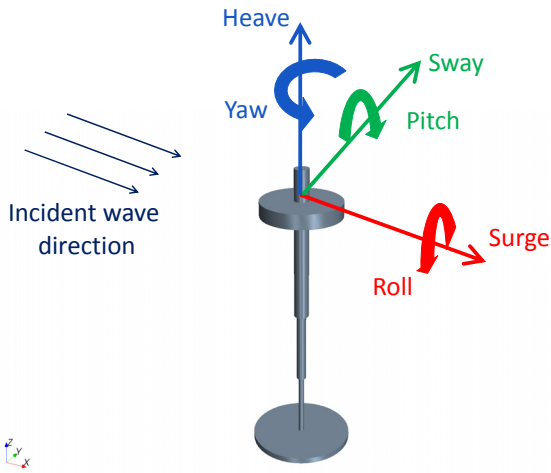


FIGURE 3. THE TRANSLATION AND ROTATION OF THE BODY (6 DEGREES OF FREEDOM)

Numerical wave tank settings

The domain and the domain boundaries of the numerical wave tank are plotted in Fig. 4, where the water depth is 70 m. To reduce the size of the problem, a symmetric boundary is applied along the x - y plane. The given computational domain is 100 m wide ($0m \leq y \leq 100m$); 170 m high ($-70m \leq z \leq 100m$); 7 wavelengths long ($-2\lambda \leq x \leq 5\lambda$) in the regular wave analysis and 9 wavelengths long ($-2\lambda \leq x \leq 8\lambda$) in the irregular wave analysis. The wall width to FPA diameter radius is around 19. The effect of wave reflection from the side wall is assumed to be small in this study. However, more studies need to be performed to quantify the impacts. The incident wave condition is specified at the inflow boundary, and a sponge-layer method is applied by placing a damping zone (2λ in the wave propagation direction) in front of the down wave boundary in order to

absorb the outgoing and reflecting waves without creating additional numerical disturbance. Note that the sponge-layer damping zone method has been tested. It successfully absorbs the waves in a numerical wave tank without the presence of the absorber.

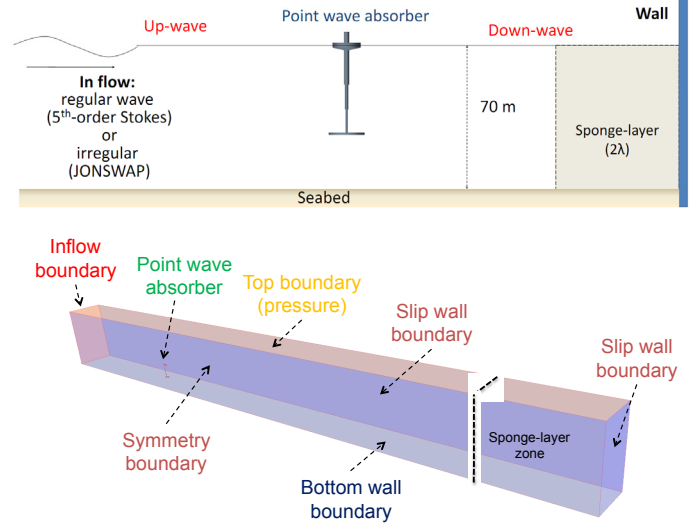


FIGURE 4. COMPUTATIONAL DOMAIN AND BOUNDARIES OF THE NUMERICAL WAVE TANK

MOORING CONFIGURATION

The FPA is connected to a mooring system to contain its horizontal and rotational motions. We are not trying to model a particular mooring system in this study. For design and optimization purposes, we use OrcaFlex to conduct the mooring line configuration study, which is a fully 3D time domain fluid and structural dynamic modeling tool. It has widely been used for modeling the dynamics of the offshore systems. The excitation forces on the absorber include the buoyancy force and the hydrodynamic wave loads that are calculated through the use of Morison's equation. The dynamics of the absorber and the mooring system are then modeled using a finite element method. The drag and added-mass coefficients for the Morison's equation are given based on [19]. Note that the effects of wave diffraction and radiation as well as the nonlinear interaction between waves and the floating body are not considered in the modeling. Although OrcaFlex has its limitations, it can provide us first-cut results in a very short time.

Based on the approach used by Fitzgerald and Bergdahl [20], and after running a series of OrcaFlex simulations with various mooring configurations, we present an "acceptable" mooring design (Fig. 5), for which the deviation of pitch is less than 25 degrees. The FPA model is connected to eight mooring lines that are divided into two layers. Each layer has four lines in the configuration of a cross, and each mooring line is connected to a spring system. The spring stiffness is equal to 160kn/m and is determined based on a series of OrcaFlex runs.

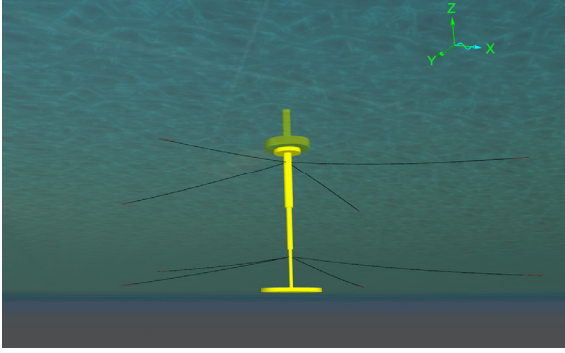


FIGURE 5. MOORING CONFIGURATION IN ORCAFLEX MODELING

In the RANS simulation, the sway, roll and yaw motions are constrained, and the FPA is only allowed to move freely in surge, heave, and pitch. The mooring system is designed based on the one used in the OrcaFlex modeling. Given that a symmetry boundary is applied, only four mooring lines are specified along the symmetry boundary in the RANS simulation (Fig. 6).

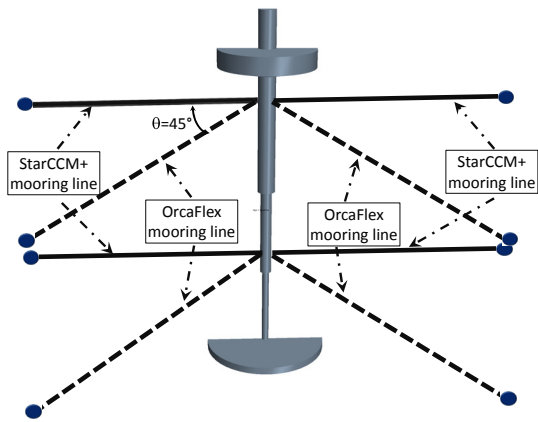


FIGURE 6. MOORING CONFIGURATION IN RANS MODELING

RANS SIMULATION

To model the details of the flow around the FPA, including wave overtopping and the nonlinear interaction between waves and the moored FPA, we utilized the RANS method. The FPA wave energy system is analyzed in both regular and irregular waves, where a 5th-order Stokes wave with a height of 10 m is applied for the regular wave study and a JONSWAP spectrum wave is applied for the irregular analysis.

Meshing

As shown in Fig. 7, the mesh is finer near the free surface in order to capture the wave dynamics and has a higher resolution around the FPA to model the details of the flow around it and its interaction with waves. In addition, prism-layer cells are placed along the FPA surface so that y^+ satisfies the turbulence model requirement.

The grid size Δx (in the wave propagation direction) is adjusted with the incident wavelength, and it is smaller than $\lambda/80$. The grid size Δz (in the vertical direction) near the free surface is in the range between $H/10$ and $H/20$, where H is the wave height. The total number of cells is on the order of 0.7 million for the regular wave analysis and 1.5 million for the irregular wave analysis.

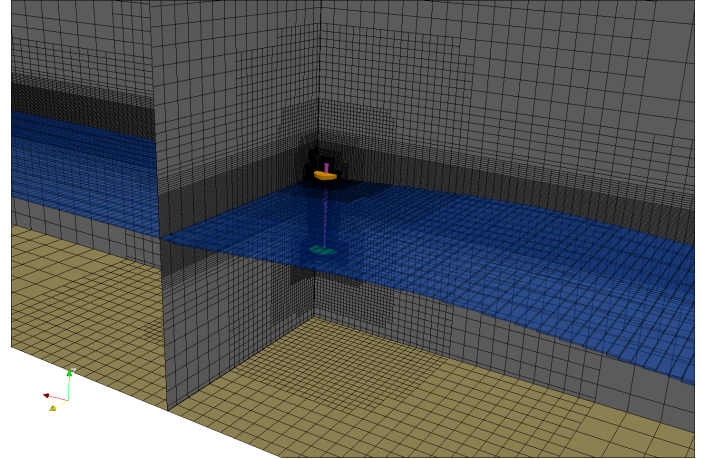


FIGURE 7. MESH AROUND THE POINT WAVE ABSORBER MODEL

In addition, a very small time step is utilized to avoid highly distorted cells, created by the morphing model due to the large movement of the FPA at each time step. The time step size is also given based on the incident wave period, and it is approximately $T/300$ in the regular wave analysis and $T_p/600$ in the irregular wave analysis, where T and T_p are the period and the peak period for the regular and irregular waves, respectively.

All the RANS simulations are carried out on NREL's high-performance computing (HPC) system. Each compute node consists of dual socket/quad-core 2.93 GHz Intel Nehalem processor with 12 GB of memory shared by all 8 cores. It takes about 8 hrs on 64 cores to complete 10 wave periods of time (approximately 3,200 time steps) for the regular wave analysis and 36 hrs on 128 cores to complete 15 peak wave periods of time (approximately 10,000 time steps) for the irregular wave analysis.

Long linear wave comparison

For long linear waves, the comparison of the heave and surge motions of the FPA are plotted in Fig. 8, which shows the results from the RANS method and OrcaFlex are in good agreement. When the wave is linear and the wave period is large, the vertical component of the excitation force is dominated by the buoyancy force, and the horizontal component is determined by the hydrodynamic wave loads. The buoyancy force is proportional to the immersed volume of the FPA, and the hydrodynamic wave loads in the horizontal direction can be calculated accurately through the use of Morison's equation because the size of the FPA is much smaller

than the incident wavelength and wave overtopping barely occurs.

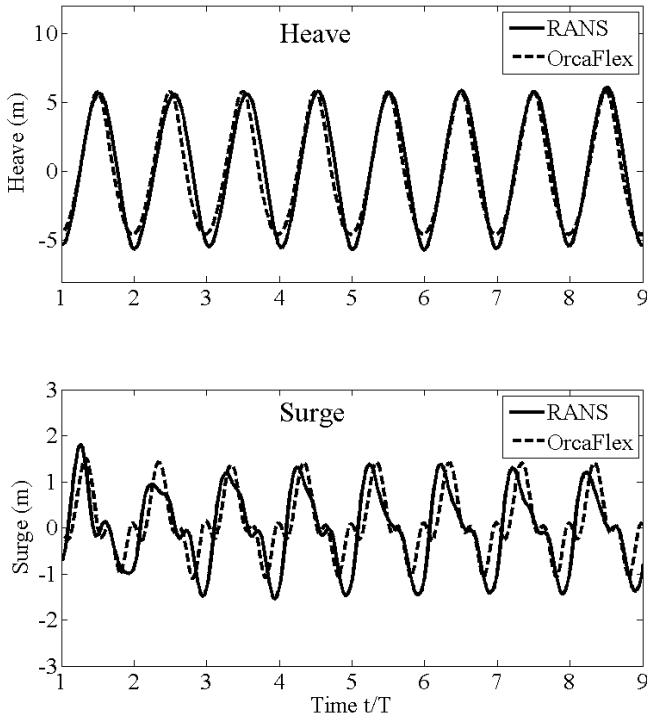


FIGURE 8. COMPARISON OF THE HEAVE AND SURGE MOTIONS FROM RANS AND ORCAFLEX (T=17.5 SEC)

Regular wave analysis

The response amplitude operators (RAOs) obtained from OrcaFlex only have good agreements with those obtained from the RANS method when the wave period is larger than 17 sec (Fig. 9). When the wave period is small, the RAOs predicted by the RANS method are smaller than those predicted by OrcaFlex. As opposed to the OrcaFlex results, the RANS solutions do not experience a resonance period in heave, at least within the range of wave periods that are studied. As shown in [18], the heave motion of the FPA generally follows the wave elevation when the incident wave period is sufficiently larger than the body natural period. When incident wave period decreases, the phase shift between the wave elevation and the FPA heave motion increases. As a result, the waves are more likely to overtop the FPA model (Fig. 10), particularly in extreme wave scenarios, where a wave with a height of 10 m is generally nonlinear when the wave period is smaller than 11 sec. In addition, flow separation is observed around the float and the reaction plate in the RANS simulation. These nonlinear effects generally provide additional damping that constrains the FPA motions.

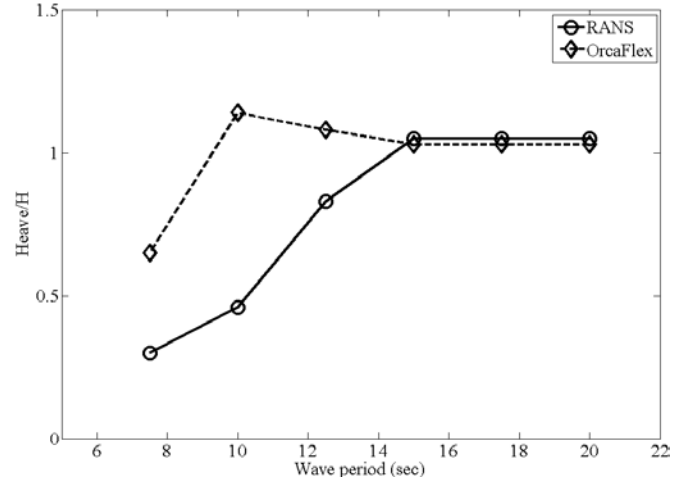


FIGURE 9. COMPARISON OF RAOs FROM RANS AND ORCAFLEX

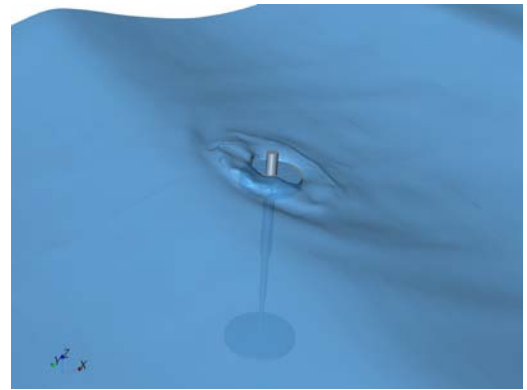


FIGURE 10. THE POINT WAVE ABSORBER MODEL IN WAVES (T=7.5SEC)

Figure 11 plots the surge and pitch of the FPA in waves. The surge response is in the range between 3 m and 6 m, and the pitch angle is around 5 degrees. Both the surge and the pitch increase slightly as the wave period decreases.

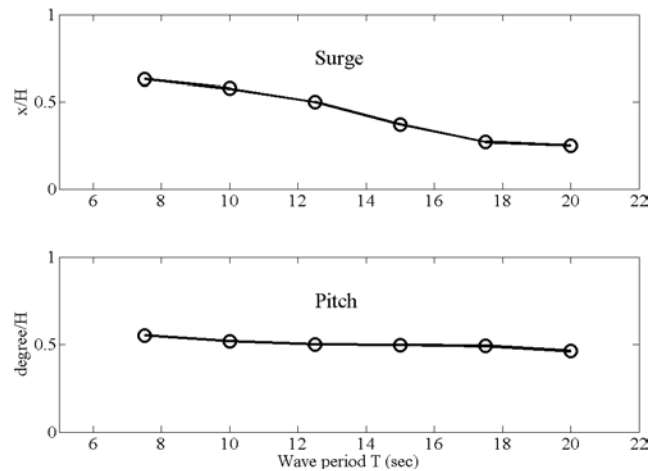


FIGURE 11. SURGE AND PITCH MOTIONS OF THE FPA MODEL FROM RANS SIMULATIONS

Figure 12 shows the hydrodynamic pressure distribution near the FPA model at a time instant of $t/T=7.65$, and Figure 13 plots the pressure distributions on the FPA surface at three time instants. Note that the absorber is subject to a wave at its peak at $t/T=10.49$, and at its trough at $t/T=9.99$. Because the motion of fluid particles decreases rapidly with increasing depth below the free surface, the hydrodynamic wave impact on the float is more significant than that on the reaction plate.

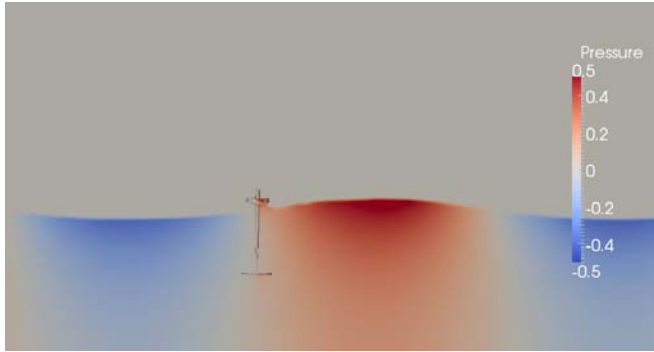


FIGURE 12. HYDRODYNAMIC PRESSURE (SCALED BY $\rho g D$) CONTOUR AROUND FPA ($T=12.5\text{SEC}$; $H=10\text{M}$)

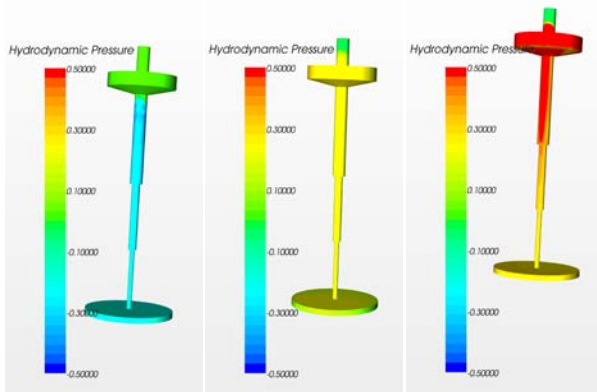


FIGURE 13. THE PRESSURE DISTRIBUTION ON THE FPA SURFACE AT $t/T=9.99$ (LEFT), $t/T=10.32$ (MIDDLE), AND $t/T=10.49$ (RIGHT) ($T=12.5\text{SEC}$)

The corresponding horizontal and vertical forces, including the buoyancy force, wave impact, and the weight of the FPA device are plotted in Fig. 14. Given that the fluid particle velocity is proportional to the incident wave frequency, the forces increase as the incident wave period decreases as expected. The forces on the FPA body under extreme wave conditions are useful information for further cost assessment.

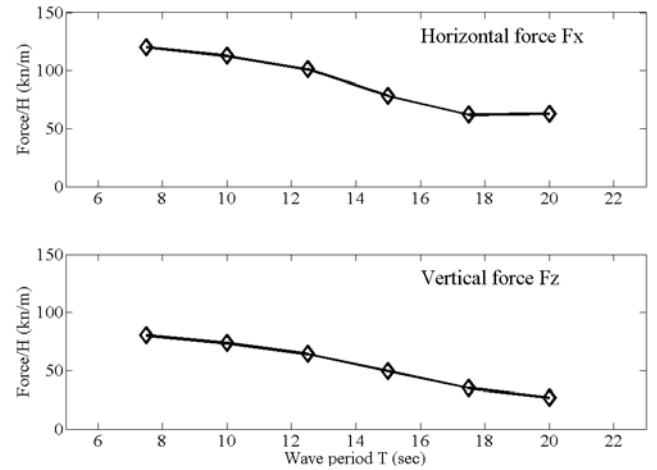


FIGURE 14. HORIZONTAL AND VERTICAL FORCES ON THE FPA

Irregular wave analysis

In our irregular wave analysis, we only present a scenario where the FPA is modeled using a JONSWAP spectrum wave with a significant wave height of 10 m and a peak period of 17.5 sec. The corresponding hydrodynamic response histories from the RANS method are shown in Fig. 15. The maximum heave motion is on the order of the maximum wave height. We plan to conduct a more detailed analysis with a longer period of simulation and various wave conditions in the future.

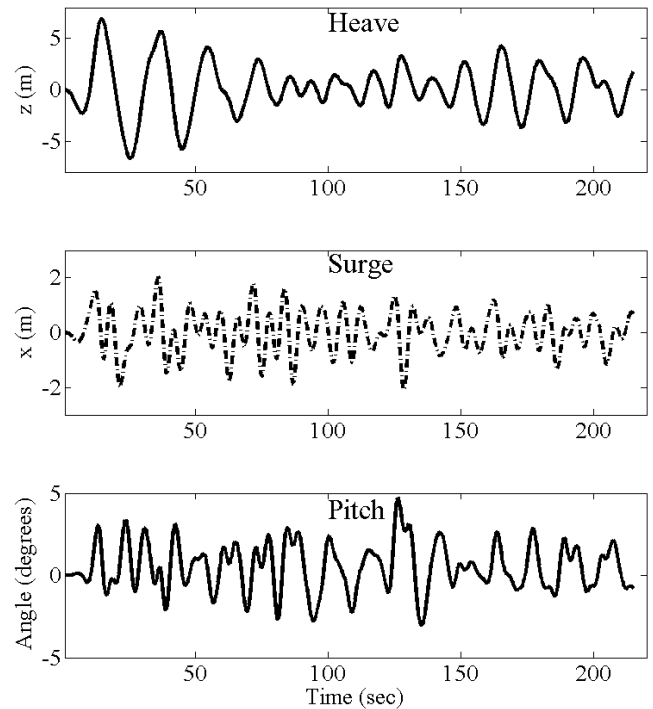


FIGURE 15. FPA HYDRODYNAMIC RESPONSE IN JONSWAP SPECTRUM WAVES

DISCUSSIONS

As the wave period decreases, the phase shift between the FPA heave motion and the wave elevation increases. Therefore, the nonlinear interaction between waves and the FPA device becomes more significant, especially in small wave period and large wave height scenarios. As a result, the additional damping forces, including those due to flow separation and wave overtopping, limit the motion of the FPA, particularly under the extreme wave conditions.

The Morison's equation prediction is expected to be applicable when the wave is linear. However, for some linear wave scenarios, the OrcaFlex results are deviated from the RANS simulations, as shown in Fig. 9. In addition to the aforementioned nonlinear effects, the relationship between the buoyancy force and the hydrodynamic wave loads and the feasible values of the added-mass and damping coefficients for predicting the excitation force of this particular FPA geometry require further investigation, particularly in the body axial direction. A more rigorous method is to compute the hydrodynamic coefficients through the use of a potential flow method.

Although using OrcaFlex for predicting the FPA motions has its limitations, OrcaFlex is still an efficient numerical tool that provides us with a very useful first-cut analysis, particularly for small amplitude linear wave scenarios. The computational cost for running such a design and optimization tool is small. On the other hand, under extreme wave conditions, the hydrodynamics of a FPA is complex. The interaction between waves and the moored FPA is often fully nonlinear, and wave overtopping often occurs. Therefore, the use of RANS models is suggested.

CONCLUSIONS

In this paper, we presented the results of our study of the hydrodynamics of a moored FPA in extreme wave conditions. We analyzed the baseline mooring configuration using OrcaFlex and modeled the detail of the flow using a RANS method. The study shows that waves often overtop the FPA when the FPA is under extreme wave conditions. The FPA motions are constrained by the effects of viscous damping as well as the nonlinear interaction between waves and the moored FPA. Furthermore, through a few irregular wave simulations, we find that the maximum heave motion of the FPA is on the order of the maximum wave height, although more simulations are needed to confirm this. Overall, we found our mooring line design to be effective. We also found that the Morison's Equation method can be only used for a very few scenarios and with caution for extreme wave scenarios analyses.

FUTURE WORK

With all the promising results presented here, we intend to continue our research with the following efforts:

- Conduct a more comprehensive irregular wave analysis to understand the FPA's behavior in the open ocean environment.

- Perform a detailed analysis of the cost-effectiveness of the RANS tool to understand what setup we should use for the future design; it is still too costly even though we have access to a HPC system.
- Conduct experimental tests to validate the numerical simulation presented in this study.

REFERENCES

- [1] Thorpe, T. W., 1999. *A brief review of wave energy*. Harwell Laboratory, Energy Technology Support Unit.
- [2] Falcão, A., 2010. "Wave energy utilization: A review of the technologies," *Renewable and Sustainable Energy Reviews*, vol. 14, pp. 899-918.
- [3] Drew, B., Plummer, A., and Sahinkaya, M., 2009. "A review of wave energy converter technology," *Proceedings of the Institution of Mechanical Engineers, Part A: Journal of Power and Energy*, vol. 223, no. 8, pp. 887-902.
- [4] Budal, K. and Falnes, J., 1975. "A resonant point absorber of ocean-wave power," *Nature*, vol. 256, pp. 478-479, corrigendum 257:626.
- [5] Evans, D., 1976. "A theory for wave-power absorption by oscillating bodies," *Journal of Fluid Mechanics*, vol. 77, no. 01, pp. 1-25.
- [6] Mei, C., 1976. "Power extraction from water waves," *Journal of Ship Research*, vol. 20, pp. 63-66.
- [7] Budal, K. and Falnes, J., 1980. "Interacting point absorbers with controlled motion," *Power from sea waves*, pp. 381-399.
- [8] Falnes, J., 2002. *Ocean waves and oscillating systems*. Cambridge University Press.
- [9] Falnes, J., 2007. "A review of wave-energy extraction," *Marine Structures*, vol. 20, no. 4, pp. 185-201.
- [10] Bjarte-Larsson, T. and Falnes, J., 2006. "Laboratory experiment on heaving body with hydraulic power take-off and latching control," *Ocean Engineering*, vol. 33, no. 7, pp. 847-877.
- [11] Yavuz, H., Stallard, T., McCabe, A., and Aggidis, G., 2007. "Time series analysis-based adaptive tuning techniques for a heaving wave energy converter in irregular seas," *Proceedings of the Institution of Mechanical Engineers, Part A: Journal of Power and Energy*, vol. 221, no. 1, pp. 77-90.
- [12] Garnaud, X. and Mei, C., 2009. "Wave-power extraction by a compact array of buoys," *Journal of Fluid Mechanics*, vol. 635, pp. 389-413.
- [13] Vicente, P., Falcão, A., Gato, L., and Justino, P., 2009. "Dynamics of arrays of floating point-absorber wave energy converters with inter-body and bottom slack-mooring connections," *Applied Ocean Research*, vol. 31, pp. 267-281.

- [14] McCabe, A., Bradshaw, A., Meadowcroft, J., and Aggidis, G., 2006. "Developments in the design of the PS Frog Mk 5 wave energy converter," *Renewable Energy*, vol. 31, no. 2, pp. 141-151.
- [15] Cruz, J. and Salter, S., 2006. "Numerical and experimental modelling of a modified version of the Edinburgh Duck wave energy device," *Proceedings of the Institution of Mechanical Engineers, Part M: Journal of Engineering for the Maritime Environment*, vol. 220, no. 3, pp. 129-147.
- [16] Mavrakos, S. and Kalofonos, A., 1997. "Power absorption by arrays of interacting vertical axisymmetric wave-energy devices," *Journal of Offshore Mechanics and Arctic Engineering*, vol. 119, p. 244.
- [17] Agamloh, E., Wallace, A., and Von Jouanne, A., 2008. "Application of fluid-structure interaction simulation of an ocean wave energy extraction device," *Renewable Energy*, vol. 33, no. 4, pp. 748-757.
- [18] Yu, Y.-H. and Li, Y., 2011. "A RANS Simulation for the Heave Response of a Two-Body Floating Point Wave Absorber," Proceedings of the 21st International Offshore (Ocean) and Polar Engineering Conference, ISOPE, Maui, Hi, USA.
- [19] Sarpkaya, T., 2010. *Wave forces on offshore structures*. Cambridge University Press.
- [20] Fitzgerald, J. and Bergdahl, L., 2008. "Including moorings in the assessment of a generic offshore wave energy converter: A frequency domain approach," *Marine Structures*, vol. 21, no. 1, pp. 23-46.